Noise and pattern formation in periodically driven Rayleigh-Bénard convection

Omar Osenda and Carlos B. Briozzo
Facultad de Matemática, Astronomía y Física, Universidad Nacional de Córdoba, 5000 Córdoba, Argentina

Manuel O. Cáceres
Centro Atómico Bariloche, Comisión Nacional de Energía Atómica, 8400 San Carlos de Bariloche, Argentina
(Received 26 June 1997)

We present a new model for periodically driven Rayleigh-Bénard convection with thermal noise, derived as a truncated vertical mode expansion of a mean field approximation to the Oberbeck-Boussinesq equations. The resulting model includes the continuous dependence on the horizontal wave number, and preserves the full symmetries of the hydrodynamic equations as well as their inertial character. The model is shown to reduce to a Swift-Hohenberg-like equation in the same limiting cases in which the Lorenz model reduces to an amplitude equation. The order-disorder transition experimentally observed in the recurrent pattern formation near the convective onset is studied by using both the present model and its above-mentioned limiting form, as well as a generalization of the amplitude equation for modulated driving introduced by Schmitt and Lücke [Phys. Rev. A **44**, 4986 (1991)] and the generalized Lorenz model previously introduced by the authors [Phys. Rev. E **55**, R3824 (1997)]. We show that all these models agree with the experimental data much closer than previous models like the Swift-Hohenberg equation or the amplitude equation, though thermal noise alone still seems insufficient to lead to a precise fit. The relationship between these models is discussed, and it is shown that the inclusion of the continuous wave-number dependence, a consistent treatment of the driving time dependence, and the inclusion of inertial effects are all relevant to the formulation of a model describing equally well both the time-periodic and static driving cases. [S1063-651X(97)09812-7]

PACS number(s): 47.20.Bp, 05.40.+j, 47.20.Hw, 02.50.Ey

I. INTRODUCTION

Pattern formation outside of equilibrium has become a very active field in the past several years [1], in part pushed forward by the advancement of experimental techniques allowing the realization of quantitative experiments [2–6], and in part by the continuing development of theoretical models [7–13]. In particular, Rayleigh-Bénard convection (RBC) has become a paradigm in the study of complex spatiotemporal behavior of nonequilibrium systems.

The role of fluctuations in the initial stages of pattern formation was recognized early on as deserving detailed examination [7]. Fluctuations in RBC below but not too near the convection threshold can be considered to be currently well understood, both qualitative and quantitatively [5]. This understanding has been facilitated by the fact that, below threshold, the hydrodynamic equations can to a very good approximation be linearized around the conductive state, and linear response theory applied. The same could in principle be done well above threshold, by linearizing around a well-developed (macroscopic) convective state which satisfies the nonlinear deterministic equations [14], though we are unaware of any works implementing this approach in the literature. The situation very close to threshold is far less clear, since there the linear and nonlinear terms and the thermal fluctuations are all of comparable importance. In particular, the effects of noise can be expected to be relevant in the *dynamic* onset of convection, when a system is swept through the convection threshold by externally modulating the control parameter.

A time-honored experiment still waiting for a full theoretical explanation is the one performed by Meyer, Ahlers, and Cannell [3]. In this experiment the Rayleigh number R (the control parameter) of a Rayleigh-Bénard cell was modulated in time as $R(t)/R_c - 1 = \epsilon_0 + \delta \cos(\omega t)$, periodically crossing the static convection threshold $R = R_c$. The modulation was selected such that in each period a well-developed convective pattern was established and subsequently nearly or completely vanished. It was observed that depending on the values of the experimental parameters the system presented an order-disorder transition, between situations in which the same pattern reappeared at each cycle (*deterministic state*), and situations in which the patterns at successive cycles were uncorrelated (*stochastic state*). This change in behavior defined an order-disorder transition line (ODTL) in the ϵ_0-δ plane.

In the intervening years a number of models have been proposed to explain this ODTL [15–19], but for all of them agreement with the experimental data was achieved only by taking the noise strength as an adjustable parameter and setting its value to be $\sim 10^4 - 10^5$ times the one computed from thermodynamic considerations [20]. All these models are based on Swift-Hohenberg (SH) or amplitude equations, and include a supercritical bifurcation at threshold, but the time modulation of the driving is incorporated *ad hoc* in these equations, originally derived for a static Rayleigh number. These models also share a purely dissipative behavior, being based on differential equations which are of first order in time. Some of them have the additional shortcoming of not respecting the full horizontal translational and rotational invariance of the hydrodynamic equations. This leads to the question of how much of their quantitative disagreement with the experimental data comes from these features.

Several years ago Ahlers, Hohenberg, and Lücke [10] for-

mulated a generalized Lorenz model for periodically driven RBC. They found that in this model the convection threshold is nontrivial, contrary to what happens with models based on SH or amplitude equations. Their model also reflected the inertial character of the hydrodynamic equations, reducing to an amplitude equation only for large Prandtl numbers (i.e., large damping) and vanishing modulation amplitude δ. This made it a good starting point for investigating the possible importance of these features for the description of the order-disorder transition. We recently extended this model by including thermal noise [13], and found that the resulting model predicted an ODTL much nearer to the experimental data of Ref. [3] than any of the previous ones, fitting the data with a noise intensity ~ 250 times the thermal one. However, this model incorporates the rather crude approximations of restricting the horizontal wave number to that of the critical mode at $R=R_c$, and imposing a parallel roll structure. As pointed out by Graham [12], in principle the rotational symmetry of the hydrodynamic equations must be broken by any emerging pattern *spontaneously* rather than by any external agent. So the question arises if it is possible to formulate a model retaining the desirable characteristics of the Lorenz model while respecting the full symmetries of the hydrodynamic equations.

The purpose of the present work is twofold. In the first place we aim to derive a model equation for periodically driven RBC which (a) respects the full (horizontal) rotational and translational invariance of the hydrodynamic equations, not imposing *a priori* any preferred convective structure; (b) preserves their main dynamical features, specifically the ''inertial'' character embedded in their structure as a *system* of differential equations of first order in time, not trivially reducible to a single first-order equation; (c) accounts for the fact that the nonlinear coupling comes (at least in part) from the interaction of the velocity and temperature fields, and not from the self-coupling of a *single* field; (d) does not project the full noise terms of the hydrodynamic equations onto their linearly most unstable mode; and (e) includes the time dependence of the control parameter *ab initio*. This is done in Sec. II, where we introduce a mean field (MF) approximation to the Oberbeck-Boussinesq (OB) equations and an expansion in vertical eigenfunctions, allowing a self-consistent calculation of the hydrodynamic fields' self- and cross-correlations, in terms of which the ODTL can be defined.

In the second place we aim to compare the main features of this model with those of previous ones, in order to shed some light on the question of which features must be incorporated in a ''good'' model equation able to account for the main physical effects present in externally modulated pattern-forming systems like the one in Ref. [3]. This is done in Sec. III, where we compare the model of Sec. II with (a) the reduction of the model of Sec. II to a Swift-Hohenberg-like equation detailed in Appendix C 1, valid for large Prandtl numbers and vanishing modulation amplitude; (b) the stochastic Lorenz model recently introduced by the authors [13]; and (c) the modulated-driving amplitude equation recently derived by Schmitt and Lücke [11], which we extend to include noise in Appendix C 2. We pay special attention to the noise and nonlinear coupling terms of these model equations, and discuss both the technical and physical validity of the approximations introduced in the derivation of the model in Sec. II. With the aim of increasing legibility, most of the calculations have been deferred to the appendixes.

II. MODEL

A. Fundamental equations

We consider a fluid layer between two laterally infinite horizontal plates ($-\infty \leqslant x,y \leqslant \infty$) separated by a distance d, and having a time-dependent temperature difference which will be the control parameter driving the system. The density of the fluid is ρ, its temperature is T, its velocity is $\mathbf{u}$, and its pressure is p. The kinematic viscosity is denoted by ν, the thermal diffusivity by κ, and the gravitational acceleration by g. We introduce dimensionless variables by the scaling $t \to (\kappa/d^2)t$, $l \to l/d$, $\Delta T \to R$, where $R=(\alpha g d^3 \Delta T)/(\kappa\nu)$ is the Rayleigh number and ΔT is the average temperature difference between the lower and upper plates. Defining the Prandtl number $\sigma=\nu/\kappa$, the Oberbeck-Boussinesq equations with noise read [10]

$$(\partial_t + \mathbf{u}\cdot\nabla)\mathbf{u} = \sigma\nabla^2\mathbf{u} + \sigma T\hat{z} - \nabla p + \nabla\cdot\mathsf{s}, \tag{1a}$$

$$(\partial_t + \mathbf{u}\cdot\nabla)T = \nabla^2 T - \nabla\cdot\mathbf{q}, \tag{1b}$$

$$\nabla\cdot\mathbf{u} = 0. \tag{1c}$$

In these equations, the effect of thermal fluctuations has been incorporated by adding the Langevin (white) noise sources s and $\mathbf{q}$ [1,9]. These are assumed to be zero-mean Gaussian noise fields with self-correlations

$$\langle s_{ij}(\mathbf{r},t)s_{lm}(\mathbf{r}',t')\rangle = c_s\delta(\mathbf{r}-\mathbf{r}')\delta(t-t')(\delta_{il}\delta_{jm}+\delta_{im}\delta_{jl}), \tag{2a}$$

$$\langle q_i(\mathbf{r},t)q_j(\mathbf{r},t)\rangle = c_q\delta(\mathbf{r}-\mathbf{r}')\delta(t-t')\delta_{ij}, \tag{2b}$$

and thermodynamic intensities

$$c_s = \left(\frac{k_B T}{\rho d\nu^2}\right)2\sigma^3, \quad c_q = \frac{2(Td^3\alpha g/\kappa\nu)^2}{(c_V d^3/k_B)}. \tag{3}$$

For the velocity field, we will assume *rigid* vertical boundary conditions (BC's)

$$\mathbf{u} = \mathbf{0}, \quad z = \pm\tfrac{1}{2}, \tag{4}$$

more realistic than the technically simpler free-slip BC's. Note that Eq. (1c) then implies $\partial_z u_z = 0$ at $z=\pm\frac{1}{2}$.

For the temperature field, we will assume the same *perfect thermal contact* BC's at $z=\pm\frac{1}{2}$ as in the experimental setting of Meyer, Ahlers, and Cannell [3]: the temperature of the upper plate will be taken as constant, while that of the lower plate will have a time-periodic modulation. The dimensionless temperature T in Eqs. (1) is more conveniently expressed as

$$T(\mathbf{r},t) = T^c(z,t) + \theta(\mathbf{r},t) \tag{5}$$

in terms of the instantaneous conduction profile T^c satisfying the heat conduction equation

$$\partial_t T^c = \partial_z^2 T^c. \tag{6}$$

The periodic driving is accounted for by the BC's

$$T^c(-\tfrac{1}{2},t)=T^l(t)=T_l+\Delta\ \cos(\omega t), \tag{7a}$$

$$T^c(\tfrac{1}{2},t)=T^u(t)=T_u\,. \tag{7b}$$

The deviation θ from the conduction profile then vanishes at $z=\pm\frac{1}{2}$. Defining the time-dependent Rayleigh number

$$R(t)=T^l(t)-T^u(t)=T_l-T_u+\Delta\ \cos(\omega t), \tag{8}$$

the conduction profile can in turn be separated as

$$T^c(z,t)=T_u+(\tfrac{1}{2}-z)R(t)+S(z,t), \tag{9}$$

where $T_u+(1/2-z)R(t)$ is an instantaneous *linear* profile, and $S(z,t)$ is a deviation from linearity which vanishes only for static driving $\Delta=0$ (see Appendix B 1 for full details).

Applying the transverse projection operator $\nabla\times\nabla\times$ to Eq. (1a), and using Eq. (1c), the pressure term is eliminated and the OB equations are rewritten as

$$\partial_t\partial_j\partial_j u_i=\sigma\partial_j\partial_j\partial_k\partial_k u_i+\sigma(\delta_{iz}\partial_j\partial_j-\partial_i\partial_z)\theta+(\partial_i\partial_j\partial_k-\delta_{ij}\partial_l\partial_l\partial_k)(u_j u_k-s_{jk}), \tag{10a}$$

$$\partial_t\theta=\partial_j\partial_j\theta-u_z\partial_z T^c-\partial_j(\theta u_j+q_j)\,, \tag{10b}$$

where $i,j,k,l=x,y,z$ (sum over repeated indexes is understood). The (rigid) BC's for these equations are

$$u_x=u_y=u_z=\partial_z u_z=\theta=0,\quad z=\pm\tfrac{1}{2}. \tag{11}$$

B. Mean field approximation

Let's make some considerations about the properties of the averages of the fields u_i and θ over the ensemble of realizations of the noises q_i and s_{ij}. First we note that the horizontal translational and rotational symmetry of the differential operators in Eqs. (10), together with the statistical spatial homogeneity of the white noise fields, insure that the stochastic fields u_i and θ are homogeneous in the horizontal coordinates. Having a laterally infinite system further insures that every spatially inhomogeneous configuration of the hydrodynamic fields, will appear with equal probability at every possible orientation and horizontal offset. Thus we have

$$\langle u_i\rangle=0 \tag{12}$$

and

$$\langle\theta\rangle,\quad\langle\theta^2\rangle,\quad\langle\theta u_i\rangle,\quad\langle u_i u_j\rangle\quad\text{independent of } x,y, \tag{13}$$

for $i,j=x,y,z$, either in the macroscopic conductive or convective states. Using these results, averaging Eqs. (10), and remembering that differentiation operators can be taken outside the ensemble averages, we obtain

$$0=\delta_{iz}\partial_z^3\langle u_z^2\rangle-\partial_z^3\langle u_i u_z\rangle, \tag{14a}$$

$$\partial_t\langle\theta\rangle=\partial_z^2\langle\theta\rangle-\partial_z\langle\theta u_z\rangle. \tag{14b}$$

Equation (14a) reduces to an identity for $i=z$, so it does not impose any restriction on $\langle u_z^2\rangle$. For $i=x,y$ it reduces to

$$\partial_z^3\langle u_x u_z\rangle=\partial_z^3\langle u_y u_z\rangle=0, \tag{15}$$

so $\langle u_x u_z\rangle$ and $\langle u_y u_z\rangle$ must be quadratic functions of z. The rigid boundary conditions $u_x=u_y=u_z=\partial_z u_z=0$ at $z=\pm\frac{1}{2}$ then impose

$$\langle u_x u_z\rangle=\langle u_y u_z\rangle=0. \tag{16}$$

Equation (14b) will be used as a self-consistency condition in what follows.

We now introduce a MF approximation to Eqs. (10), based on the preceding cosiderations. Note that in Eqs. (1) the *only* nonlinear terms come from the material derivative $\mathbf{u}\cdot\nabla$. The usual way to linearize these equations is discarding these terms by approximating $\mathbf{u}\cdot\nabla u_j$ and $\mathbf{u}\cdot\nabla\theta$ by zero, i.e., one linearizes around the conductive state. This enhances greatly the solvability of the equations, but it is clearly a dissatisfying approximation for a system that can be, at least at some times, in a fully developed convective state. The MF approximation consists in approximating these terms by the *ensemble average* values of the corresponding fields, that is

$$\mathbf{u}\cdot\nabla u_i\to\mathbf{u}\cdot\nabla\langle u_i\rangle, \tag{17a}$$

$$\mathbf{u}\cdot\nabla\theta\to\mathbf{u}\cdot\nabla\langle\theta\rangle \tag{17b}$$

(note that we do *not* approximate the material derivative operator itself). This is in the same spirit of the usual mean field approximation of statistical mechanics, which assumes that the only important configuration near a critical point is the spatially uniform one [21]. For the ensemble averages we have $\langle u_i\rangle=0$, so in this approximation Eqs. (10) read

$$\partial_t\partial_j\partial_j u_i=\sigma\partial_j\partial_j\partial_k\partial_k u_i+\sigma(\delta_{iz}\partial_j\partial_j-\partial_i\partial_z)\theta-(\partial_i\partial_j\partial_k-\delta_{ij}\partial_l\partial_l\partial_k)s_{jk}, \tag{18a}$$

$$\partial_t\theta=\partial_j\partial_j\theta-u_z\partial_z T^c-\partial_j(\langle\theta\rangle u_j+q_j). \tag{18b}$$

We must stress that this is an *uncontrolled* approximation (as is the usual linearization around $\mathbf{u}=\mathbf{0}$), whose accuracy must be checked *a posteriori* against the results of the corresponding full equations in all cases where the last can be solved.

The pair of equations for u_z and θ in Eqs. (18) is now closed, and we will henceforth work with the systems

$$\partial_t\nabla^2 u_z=\sigma\nabla^4 u_z+\sigma\nabla_\perp^2\theta+\mathcal{S}_z(\mathbf{r},t), \tag{19a}$$

$$\partial_t\theta=\nabla^2\theta-u_z\partial_z(T^c+\langle\theta\rangle)+\mathcal{Q}(\mathbf{r},t), \tag{19b}$$

where we used that $\partial_j u_j=0$ and $\langle\theta\rangle=\langle\theta(z,t)\rangle$, and defined $\nabla_\perp^2=\partial_x^2+\partial_y^2$. The noises $\mathcal{S}_z$ and $\mathcal{Q}$ are defined as

$$\mathcal{S}_z(\mathbf{r},t)=(\delta_{zj}\nabla^2\partial_k-\partial_z\partial_j\partial_k)s_{jk}\,, \tag{20a}$$

$$\mathcal{Q}(\mathbf{r},t)=-\partial_j q_j\,, \tag{20b}$$

and it is fairly direct to show (see Appendix B 2) that

$$\langle\mathcal{S}_z(\mathbf{r},t)\mathcal{Q}(\mathbf{r}',t')\rangle=\langle\mathcal{S}_z(\mathbf{r},t)\rangle=\langle\mathcal{Q}(\mathbf{r},t)\rangle=0, \tag{21a}$$

$$\langle \mathcal{S}_z(\mathbf{r},t)\mathcal{S}_z(\mathbf{r}',t')\rangle = -c_s\delta(t-t')\nabla^4\nabla_\perp^2\delta(\mathbf{r}-\mathbf{r}'), \tag{21b}$$

$$\langle \mathcal{Q}(\mathbf{r},t)\mathcal{Q}(\mathbf{r}',t')\rangle = -c_q\delta(t-t')\nabla^2\delta(\mathbf{r}-\mathbf{r}') \tag{21c}$$

for any set of test functions satisfying the BC's (11). Considering $\langle\theta\rangle$ as a given function of z and t to be determined *a posteriori*, Eqs. (19) can be regarded as a system of *linear* stochastic partial differential equations which, though complicated, is amenable to standard analysis techniques.

C. Truncated expansion in vertical eigenfunctions

We now introduce an expansion of the fields $u_z(\mathbf{r},t)$ and $\theta(\mathbf{r},t)$ in vertical eigenfunctions $U_{zn}(z)$ and $\Theta_n(z)$. These eigenfunctions are obtained in Appendix A as static solutions of the linear, noiseless OB equations (10). As shown in Appendix A, these eigenfunctions have definite parity in z, and their correct orthonormality relations are

$$\int_{-1/2}^{1/2} U_{zn}(z)\Theta_m(z)dz = \delta_{nm}, \tag{22}$$

but $\int_{-1/2}^{1/2}U_{zn}(z)U_{zm}(z)dz$ and $\int_{-1/2}^{1/2}\Theta_n(z)\Theta_m(z)dz$ are nonvanishing except by parity.

Closely following the derivation of the Lorenz model [10,13], we retain only the lowest vertical modes leading to a nontrivial approximation, setting

$$u_z(\mathbf{x},z,t) \simeq \overline{u_{z0}}(\mathbf{x},t)U_{z0}(z), \tag{23a}$$

$$\theta(\mathbf{x},z,t) \simeq \overline{\theta_0}(\mathbf{x},t)\Theta_0(z) + \overline{\theta_1}(\mathbf{x},t)\Theta_1(z), \tag{23b}$$

$$T^c(z,t) \simeq T_u + (1/2-z)R(t) + \Theta_0(z)S_0(t) + \Theta_1(z)S_1(t), \tag{23c}$$

where $\mathbf{x}=(x,y)$, and we replaced $S(z,t)$ in the conductive profile by its expansion

$$S(z,t) \simeq \Theta_0(z)S_0(t) + \Theta_1(z)S_1(t) \tag{24}$$

which is worked out in detail in Appendix B 1. Defining the inner product $\{fg\}=\int_{-1/2}^{1/2}f(z)g(z)dz$, substituting expansion (23) in Eqs. (19) and in the consistency condition (14b), and using the parity and orthonormality of the eigenfunctions, we obtain

$$\partial_t(\nabla_\perp^2 + \{\Theta_0 U_{z0}''\})\,\overline{u_{z0}} = \sigma(\nabla_\perp^4 + 2\{\Theta_0 U_{z0}''\}\nabla_\perp^2 + \{\Theta_0 U_{z0}^{iv}\})\,\overline{u_{z0}} + \sigma\{\Theta_0\Theta_0\}\nabla_\perp^2\,\overline{\theta_0} + \{\Theta_0\mathcal{S}_z\}, \tag{25a}$$

$$\partial_t\,\overline{\theta_0} = (\nabla_\perp^2 + \{U_{z0}\Theta_0''\})\,\overline{\theta_0} + [\{U_{z0}U_{z0}\}R(t) - (S_1(t) + \langle\,\overline{\theta_1}\rangle)\{U_{z0}U_{z0}\Theta_1'\}]\,\overline{u_{z0}} + \{U_{z0}\mathcal{Q}\}, \tag{25b}$$

$$\partial_t\langle\,\overline{\theta_1}\rangle = \{U_{z1}\Theta_1''\}\langle\,\overline{\theta_1}\rangle - \{U_{z1}(\Theta_0 U_{z0})'\}\langle\,\overline{\theta_0}\,\overline{u_{z0}}\rangle, \tag{25c}$$

where the primes denote derivatives with respect to z. Note that the fundamental mode $S_0(t)$ of $S(z,t)$ does not enter these equations.

Fourier transforming from $\mathbf{x}$ to $\mathbf{k}$, and performing several partial integrations to symmetrize the inner products, we arrive at

$$\partial_t\widetilde{u}_{z0} = -\sigma\frac{k^4 + 2\{U_{z0}'\Theta_0'\}k^2 + \{\Theta_0 U_{z0}^{iv}\}}{k^2 + \{U_{z0}'\Theta_0'\}}\widetilde{u}_{z0} + \sigma\frac{\{\Theta_0\Theta_0\}k^2}{k^2 + \{U_{z0}'\Theta_0'\}}\widetilde{\theta}_0 + \sqrt{D_u(k)}\,\widetilde{\xi}_u(\mathbf{k},t), \tag{26a}$$

$$\partial_t\widetilde{\theta}_0 = -(k^2 + \{U_{z0}'\Theta_0'\})\,\widetilde{\theta}_0 + [\{U_{z0}U_{z0}\}R(t) - \{U_{z0}U_{z0}\Theta_1'\}(S_1(t) + \langle\,\overline{\theta_1}\rangle)]\,\widetilde{u}_{z0} + \sqrt{D_\theta(k)}\,\widetilde{\xi}_\theta(\mathbf{k},t), \tag{26b}$$

$$\partial_t\langle\,\overline{\theta_1}\rangle = -\{U_{z1}'\Theta_1'\}\langle\,\overline{\theta_1}\rangle + \{U_{z0}\Theta_0 U_{z1}'\}\langle\,\overline{\theta_0}\,\overline{u_{z0}}\rangle, \tag{26c}$$

where $\widetilde{u}_{zj}(\mathbf{k},t)$ and $\widetilde{\theta}_j(\mathbf{k},t)$ denote the Fourier transforms of the fields $\overline{u_{zj}}(\mathbf{x},t)$ and $\overline{\theta_j}(\mathbf{x},t)$, respectively. Note that $\{\Theta_0 U_{z0}^{iv}\}$ cannot be symmetrized to $\{U_{z0}''\Theta_0''\}$ because of nonvanishing surface terms. The symmetrization can instead be carried out for $\{\Theta_0\Theta_0^{iv}\}$ or $\{U_{z0}U_{z0}^{iv}\}$. Here $\widetilde{\xi}_u$ and $\widetilde{\xi}_\theta$ are zero-mean (complex) Gaussian white noises with correlations

$$\langle\widetilde{\xi}_\alpha^*(\mathbf{k},t)\widetilde{\xi}_\beta(\mathbf{k}',t')\rangle = \delta_{\alpha\beta}\delta(\mathbf{k}-\mathbf{k}')\,\delta(t-t') \tag{27}$$

and intensities

$$D_u(k) = (2\pi)^2 c_s k^2\frac{\{\Theta_0\Theta_0\}k^4 + 2\{\Theta_0'\Theta_0'\}k^2 + \{\Theta_0''\Theta_0''\}}{[k^2 + \{U_{z0}'\Theta_0'\}]^2}, \tag{28a}$$

$$D_\theta(k) = (2\pi)^2 c_q[\{U_{z0}U_{z0}\}k^2 + \{U_{z0}'U_{z0}'\}]. \tag{28b}$$

The relevant contribution $S_1(t)$ to the conductive profile's deviation from linearity, is given in the long-time asymptotic regime by

$$S_1(t)=\Delta\omega\{zU_{z1}\}\frac{\{U'_{z1}\Theta'_1\}\sin(\omega t)-\omega\cos(\omega t)}{\{U'_{z1}\Theta'_1\}^2+\omega^2}. \quad (29)$$

The expressions for D_u, D_θ, and S_1 are explicitly derived in Appendix B. The numerical values of the inner products appearing in Eqs. (26), (28) and (29) are given in Table II.

D. Order-disorder transition line

Let us introduce [3] the dimensionless distance to the static threshold,

$$\epsilon_0=(T_l-T_u)/R_c-1, \quad (30)$$

and the dimensionless modulation amplitude

$$\delta=\Delta/R_c, \quad (31)$$

with R_c the static critical Rayleigh number (see Appendix A). The ODTL is experimentally determined as a curve in the ϵ_0-δ plane, below which the convective pattern developing in each cycle bears little or no resemblance with the one developed in the previous cycle, whereas above this curve the convective pattern remains essentially unchanged from cycle to cycle [3]. In terms of the stochastic fields of our model, this means that in the deterministic state the velocity field is essentially time periodic with the period of the forcing, i.e.,

$$\langle\overline{u_{z0}}(\mathbf{x},t+2\pi/\omega)\,\overline{u_{z0}}(\mathbf{x},t)\rangle_{as}=\langle[\overline{u_{z0}}(\mathbf{x},t)]^2\rangle_{as}, \quad (32)$$

whereas in the stochastic state the velocity field at a given time should be uncorrelated with the field after one period of the forcing, giving

$$\langle\overline{u_{z0}}(\mathbf{x},t+2\pi/\omega)\,\overline{u_{z0}}(\mathbf{x},t)\rangle_{as}=0. \quad (33)$$

(Here the subscript ''as'' denotes that we are considering the averages in the asymptotic—long time—regime, to avoid any transient effects.) Hence if we compute $\langle\overline{u_{z0}}(\mathbf{x},t+2\pi/\omega)\,\overline{u_{z0}}(\mathbf{x},t)\rangle_{as}$ for fixed δ and increasing ϵ_0, its value will increase from 0 to $\langle[\overline{u_{z0}}(\mathbf{x},t)]^2\rangle_{as}$ as the ODTL is crossed, and the ODTL itself can be defined [13] by the value $\epsilon_0^{tr}(\delta)$ of ϵ_0 for which

$$\langle\overline{u_{z0}}(\mathbf{x},t+2\pi/\omega)\,\overline{u_{z0}}(\mathbf{x},t)\rangle_{as}=\tfrac{1}{2}\langle[\overline{u_{z0}}(\mathbf{x},t)]^2\rangle_{as}. \quad (34)$$

There is no clear-cut criterion to set the numeric factor on the right-hand side to $\frac{1}{2}$, and any other value between zero and 1 could instead be selected. However, it is found numerically that the transition from stochastic to deterministic behavior is fairly steep as a function of ϵ_0, as has already been observed for alternative analytic definitions of the ODTL such as, e.g., those of Refs. [16] and [18]. This makes the predicted ODTL relatively insensitive to the precise value of the numeric factor in Eq. (34). Moreover, taking the numeric factor to be $\frac{1}{2}$ makes our definition of the ODTL equivalent to the many different ones found in the literature [3,15,16,18]. It must be noted that the spatial average over the horizontal coordinates is unnecessary in our definition, since the self-correlations in Eq. (34) turn out to be independent of $\mathbf{x}$ because of the statistical translational invariance of Eqs. (25).

We must now obtain evolution equations for the self-correlations in (34). To this end we cast the evolution equations for $\tilde{u}_{z0}$ and $\tilde{\theta}_0$ into the form

$$\dot{x}_{\alpha\mathbf{k}}+\int\gamma_{\alpha\mathbf{k},\beta\mathbf{k}'}x_{\beta\mathbf{k}'}d^2k'=\Gamma_{\alpha\mathbf{k}}, \quad (35)$$

where $\alpha,\beta=u,\theta$, $x_{u\mathbf{k}}(t)=\tilde{u}_{z0}(\mathbf{k},t)$, and $x_{\theta\mathbf{k}}(t)=\tilde{\theta}_0(\mathbf{k},t)$. This is a direct generalization to a continuous index $\mathbf{k}$ of the usual expression [22] for a system of coupled, linear ordinary stochastic differential equations. Here $\Gamma_{\alpha\mathbf{k}}$ are zero-mean Gaussian white noises with

$$\langle\Gamma^*_{\alpha\mathbf{k}}(t)\Gamma_{\beta\mathbf{k}'}(t')\rangle=\delta(t-t')q_{\alpha\mathbf{k},\beta\mathbf{k}'}. \quad (36)$$

In our case $\gamma_{\alpha\mathbf{k},\beta\mathbf{k}'}=\gamma_{\alpha\beta}(k,t)\,\delta(\mathbf{k}-\mathbf{k}')$ and $q_{\alpha\mathbf{k},\beta\mathbf{k}'}=q_{\alpha\beta}(k)\,\delta(\mathbf{k}-\mathbf{k}')$, where

$$\gamma_{uu}(k)=\sigma\frac{k^4+2\{U'_{z0}\Theta'_0\}k^2+\{\Theta_0U^{iv}_{z0}\}}{k^2+\{U'_{z0}\Theta'_0\}}, \quad (37a)$$

$$\gamma_{u\theta}(k)=-\sigma\frac{\{\Theta_0\Theta_0\}k^2}{k^2+\{U'_{z0}\Theta'_0\}}, \quad (37b)$$

$$\gamma_{\theta u}(k,t)=-\{U_{z0}U_{z0}\}R(t)+[S_1(t)+\langle\overline{\theta_1}(t)\rangle]\{U_{z0}U_{z0}\Theta'_1\}, \quad (37c)$$

$$\gamma_{\theta\theta}(k)=k^2+\{U'_{z0}\Theta'_0\}, \quad (37d)$$

and

$$q_{\alpha\beta}(k)=\delta_{\alpha\beta}D_\alpha(k). \quad (38)$$

Then the second-order equal-times cumulants obey the evolution equations

$$\begin{aligned}\partial_t\langle\langle x^*_{\alpha\mathbf{k}}(t)x_{\beta\mathbf{k}'}(t)\rangle\rangle=&-\gamma_{\alpha\eta}(k,t)\langle\langle x^*_{\eta\mathbf{k}}(t)x_{\beta\mathbf{k}'}(t)\rangle\rangle\\&-\gamma_{\beta\eta}(k,t)\langle\langle x^*_{\eta\mathbf{k}'}(t)x_{\alpha\mathbf{k}}(t)\rangle\rangle\\&+q_{\alpha\beta}(k)\,\delta(\mathbf{k}-\mathbf{k}'),\end{aligned} \quad (39)$$

which are the corresponding generalizations to a continuous index $\mathbf{k}$ of the well-known results for discrete indexes [22]. Defining as usual the equal-time structure factors $S_{\alpha\beta}$ by

$$\langle\langle x^*_{\alpha\mathbf{k}}(t)x_{\beta\mathbf{k}'}(t)\rangle\rangle=(2\pi)^2S_{\alpha\beta}(k,t)\,\delta(\mathbf{k}-\mathbf{k}') \quad (40)$$

and noting that $S_{u\theta}=S_{\theta u}$, we see that they obey the equations

$$\partial_tS_{uu}(k,t)=-2\gamma_{uu}(k)S_{uu}(k,t)-2\gamma_{u\theta}(k)S_{u\theta}(k,t)+\frac{1}{(2\pi)^2}q_{uu}(k), \quad (41a)$$

$$\partial_tS_{u\theta}(k,t)=-\gamma_{\theta u}(k,t)S_{uu}(k,t)-[\gamma_{uu}(k)+\gamma_{\theta\theta}(k)]S_{u\theta}(k,t)-\gamma_{u\theta}(k)S_{\theta\theta}(k,t), \quad (41b)$$

$$\partial_t S_{\theta\theta}(k,t) = -2\gamma_{\theta u}(k,t)S_{u\theta}(k,t) - 2\gamma_{\theta\theta}(k)S_{\theta\theta}(k,t) + \frac{1}{(2\pi)^2}q_{\theta\theta}(k). \tag{41c}$$

Note that $S_{\alpha\beta}$ will depend on $\mathbf{k}$ only through its modulus k, at least in the long-time asymptotic regime, because of the symmetries of Eqs. (41). This equation system must be supplemented by the consistency condition (26c), which, noting that $\langle \overline{u}_{z0}\rangle = 0$, can be cast as

$$\partial_t \langle \overline{\theta}_1\rangle = -\{U'_{z1}\Theta'_1\}\langle \overline{\theta}_1\rangle + \frac{\{U_{z0}\Theta_0 U'_{z1}\}}{2\pi}\int_0^\infty S_{u\theta}(k,t)k\ dk. \tag{42}$$

Equations (41) and (42) form a closed system of integrodifferential *deterministic* equations for the equal-time structure factors. This system must be numerically solved with arbitrary initial conditions, and after reaching the long-time asymptotic regime we calculate

$$\langle [\overline{u}_{z0}(\mathbf{x},t)]^2\rangle_{\rm as} = \frac{1}{2\pi}\int_0^\infty S^{\rm as}_{uu}(k,t)k\ dk \tag{43}$$

[remember that $\langle \overline{u}_{z0}(\mathbf{x},t)\rangle = 0$) where the superscript ''as'' denotes the asymptotic form of $S_{uu}(k,t)$].

We must also find the second-order cumulants at different times. Defining the two-time structure factors by

$$\langle\langle x^*_{\alpha\mathbf{k}}(t)x_{\beta\mathbf{k}'}(t')\rangle\rangle = (2\pi)^2 S_{\alpha\beta}(k,t,t')\delta(\mathbf{k}-\mathbf{k}'), \tag{44}$$

and, using Eqs. (26), we find

$$\partial_\tau S_{uu}(k,t+\tau,t) = -\gamma_{uu}(k)S_{uu}(k,t+\tau,t) - \gamma_{u\theta}(k)S_{u\theta}(k,t+\tau,t), \tag{45a}$$

$$\partial_\tau S_{u\theta}(k,t+\tau,t) = -\gamma_{\theta u}(k,t+\tau)S_{uu}(k,t+\tau,t) - \gamma_{\theta\theta}(k)S_{u\theta}(k,t+\tau,t), \tag{45b}$$

where we used the nonanticipative character [23] of $\widetilde{u}_{z0}$ to set $\langle \widetilde{\xi}_\alpha(\mathbf{k},t+\tau)\widetilde{u}_{z0}(\mathbf{k}',t)\rangle = 0$ for $\tau > 0$. This system must be solved with initial conditions $S_{\alpha\beta}(k,t,t) = S_{\alpha\beta}(k,t)$, taking $\langle \overline{\theta}_1(t+\tau)\rangle$ in $\gamma_{\theta u}(k,t+\tau)$ to be the asymptotic solution of Eq. (42), and computing the two-time velocity correlation as

$$\langle \overline{u}_{z0}(\mathbf{x},t+\tau)\overline{u}_{z0}(\mathbf{x},t)\rangle_{\rm as} = \frac{1}{2\pi}\int_0^\infty S^{\rm as}_{uu}(k,t+\tau,t)k\ dk. \tag{46}$$

With these results, the ODTL is defined by the condition

$$\int_0^\infty S^{\rm as}_{uu}(k,T,0)k\,dk = \tfrac{1}{2}\int_0^\infty S^{\rm as}_{uu}(k,0)k\ dk, \tag{47}$$

where $T = 2\pi/\omega$.

III. RESULTS AND DISCUSSION

A. Order-disorder transition line

We used the model introduced in Sec. II to compute numerically the ODTL for parameter values corresponding to the periodic-driving experiment of Meyer, Ahlers, and Cannell [3]. We proceeded by first reducing Eqs. (41), (42), and (45) to a finite system of ordinary differential equations (ODE's), discretizing k at intervals Δk and truncating the system at a maximum value $k_{\rm max}$. The value of Δk was progressively diminished, and that of $k_{\rm max}$ increased, until further changes no longer affected the results. In our case it sufficed to take $\Delta k = 10^{-2}q_{\rm c}$ and $k_{\rm max} = 3q_{\rm c}$. It must be noted that Eqs. (41), (42), and (45) are *not* differential equations in k, the only term relating different k values being the integral of $S_{u\theta}$ in Eq. (42). As long as this integral is computed to a sufficient precision, any discretization of k is acceptable.

For given values of ϵ_0 and δ, we first integrated the ODE system corresponding to Eqs. (41) and (42), starting for simplicity each integration at $t = 0$ with null initial conditions for $S_{\alpha\beta}(k,t)$. The ODE system was integrated successively over time intervals of duration $T = 2\pi/\omega$, until the structure factors $S_{\alpha\beta}(k,(n-1)T)$ and $S_{\alpha\beta}(k,nT)$ consistently differed by less than one part in 10^{-4}, at which time we considered that the system had reached its time-periodic asymptotic regime. We then integrated the ODE system corresponding to the *full* set of equations (41), (42), and (45) over one more period, taking as initial conditions $S_{\alpha\beta}(k,nT,nT)$ for the two-time structure factors the corresponding values of their equal-time counterparts $S_{\alpha\beta}(k,nT)$. All the integrations were performed by a quality controlled fourth-order Runge-Kutta method [24] with an overall relative precision of 10^{-8}. In no case did the value of n exceed 25.

To find the ODTL, we selected several values of the driving modulation amplitude δ in the region of interest $0 \leqslant \delta \lesssim 0.5$. For each value of δ we looked for a zero crossing of

$$\frac{\int_0^\infty S^{\rm as}_{uu}(k,(n+1)T,nT)k\,dk}{\int_0^\infty S^{\rm as}_{uu}(k,nT)k\,dk} - \frac{1}{2} \tag{48}$$

by trying successive values of the mean driving ϵ_0, until its value $\epsilon_0^{\rm tr}(\delta)$ fulfilling the transition condition (47) was bracketed within an interval no larger than 0.001. The resulting ODTL is shown in Fig. 1, where we plot $\epsilon_0^{\rm tr}(\delta)$ as a function of δ. The noise intensities c_s and c_q were taken equal to their thermodynamic values (3), which, for the parameters of Ref. [3], are

$$c_s = 7.206\times 10^{-7}, \quad c_q = 3.312\times 10^{-4}. \tag{49}$$

We also set $\omega = 1$ as in Ref. [3].

B. Alternative approaches

Here we present, for comparison purposes, the ODTL's computed from two different, alternative model equations. The first one is a Swift-Hohenberg-like equation, which can be derived from Eqs. (26) as an approximate limiting form

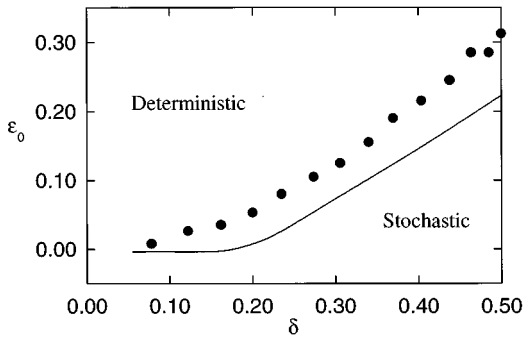

FIG. 1. Order-disorder transition line predicted by the model of this work (line). The circles are the experimental data of Meyer, Ahlers, and Cannell [3].

for large Prandtl number σ and small forcing amplitude δ. As is shown in Appendix C 1, in this case the pair of stochastic differential equations (26a) and (26b), and the consistency condition (26c), can be reduced to the single stochastic differential equation

$$\tau_0 \partial_t \overline{\psi}(\mathbf{x},t) = [(\epsilon_0+\epsilon_1)+\delta\cos(\omega t)+\epsilon_2 S_1(t) - \chi^4(\nabla^2+q_*^2)^2 - g\langle\overline{\psi^2}\rangle]\overline{\psi}(\mathbf{x},t)+\sqrt{D}\xi(\mathbf{x},t), \tag{50}$$

where $\overline{\psi}(\mathbf{x},t)=\tau_0\overline{u}_{z0}(\mathbf{x},t)$, and $\xi(\mathbf{x},t)$ is a Gaussian white noise with zero mean and

$$\langle\xi(\mathbf{x},t)\xi(\mathbf{x}',t')\rangle=\delta(\mathbf{x}-\mathbf{x}')\,\delta(t-t'). \tag{51}$$

This equation has the same form as the MF approximation to the SH equation introduced in Ref. [19]. The ODTL can be computed from this equation by the same procedure of Ref. [19]. This ODTL is shown in Fig. 2 for thermal noise intensity and parameter values corresponding to the experiments of Ref. [3], together with the one predicted by the SH equation for thermal noise.

The second alternative model equation is the amplitude equation for parallel convection rolls originally derived for free-slip BC's by Schmitt and Lücke [11], which takes into account the time-periodic driving. As shown in App. C 2, thermal noise can be incorporated into this approach in the

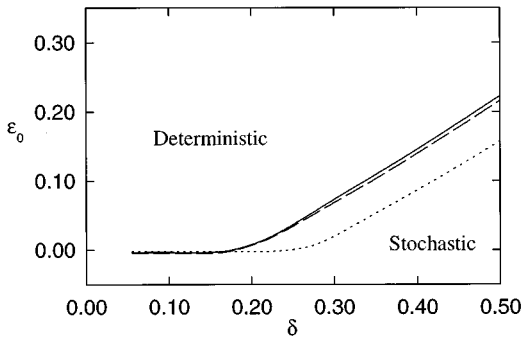

FIG. 2. Order-disorder transition line predicted by the model of this work (continuous line), its reduction to a Swift-Hohenberg-like equation (50) (dashed line), and the SH equation (dotted line).

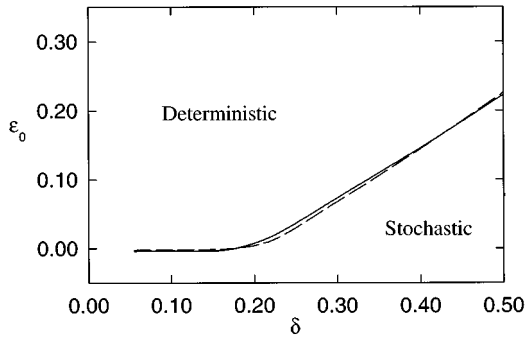

FIG. 3. Order-disorder transition line predicted by the model of this work (continuous line) and by the modulated-driving amplitude equation (52) (dashed line).

same way as is done for the static-forcing amplitude equation [8]. The MF approximation to this amplitude equation reads

$$\tau\partial_t A=[\xi^2\partial_x^2+\epsilon(t)-\epsilon_c-g\langle|A|^2\rangle]A+\xi_A(x,t), \tag{52}$$

where $A(x,t)$ is the amplitude of the vertical velocity field. The coefficients τ, ξ^2, ϵ_c, and g, and the intensity D_A of the Gaussian white noise field ξ_A, are defined in Appendix C 2 for both free-slip and rigid BC's, and $\epsilon(t)=\epsilon_0+\delta\cos(\omega t)$. The ODTL can be computed from this equation by the same procedure as for the SH equation [19]. For rigid BC's, thermal noise intensity, and parameter values corresponding to the experiments of Ref. [3], we obtain the ODTL shown in Fig. 3.

C. Comparison of models and experiment

The main formal differences between Eq. (50) and the SH equation are the nontrivial threshold ϵ_1, the presence of the extra driving term $\epsilon_2 S_1(t)$, and the displacement of the critical wave number from q_c to a near value q_*. As shown in Appendix C 1 the threshold shift ϵ_1 and the extra driving $\epsilon_2 S_1(t)$ are almost negligible for all values of the mean forcing ϵ_0 in the experiments of Meyer, Ahlers, and Cannell [3], and the critical wavelength shift amounts to less than 4%; hence these differences are not expected to be significant for the comparison with the experiments.

The parameters τ_0 and χ^2 in Eq. (50) are essentially the same as for the SH equation, as shown in Appendix C 1. This is somewhat to be expected, as these coefficients are determined by the linear stability analysis of the hydrodynamic equations. On the other hand, the parameters g and D are larger than their analogs in the SH equation. As can be seen in the derivation in Appendix C 1, their precise value depends on the scaling relating $\overline{u}_{z0}$ and $\overline{\psi}$, since they give origin to the only terms in Eq. (50) which are not homogeneous in $\overline{\psi}$. It must be noted that any such scaling leaves constant the product gD. The scaling used in writing Eq. (50) was chosen in such a way as to display explicitly the coefficients τ_0 and g in the same form as they appear in the SH equation, and with similar values.

In this context, it is worth noting that the thermal value for D in Eq. (50) exceeds the thermal noise intensity in the SH equation [1] by a factor of ~ 40, as shown in Appendix C 1. By accounting for the many horizontal modes of the

hydrodynamic equations which become linearly unstable just above the critical Rayleigh number, van Beijeren and Cohen [15] found that the effect of thermal noise on the SH equation should be enhanced over the earlier estimate by Ahlers *et al.* [2] by this same factor. The model presented here fully accounts for the linear instability at $R>R_c$ of horizontal modes with wave numbers near to but different from $k=q_c$, for the only approximation involved in deriving the noise terms and the *linear* terms of Eqs. (26a) and (26b) is the truncation of the expansion in vertical eigenfunctions. Since the vertical modes we keep are the same as in the derivation of Ref. [15], it was to be expected that we reach to a similar value for the noise intensity in a SH-like equation.

The overall properties of the amplitude equation (52) were extensively discussed in Ref. [11]. Here we will just note that, both for this equation and for the SH equation, the slope of the convective heat current as a function of the driving is known to be inversely proportional to the nonlinear coupling parameter g near the convection threshold [2,11]. As noted by Schmitt and Lücke [11], for time-periodic driving this slope is much smaller than for static driving, implying a correspondingly larger value for g. Correspondingly, the value for g in Eq. (50) is several times larger than its value for the SH equation, as shown in Appendix C 1.

By comparing Figs. 1, 2, and 3 we can see that the model introduced in this paper, its reduction to a Swift-Hohenberg-like equation, and the modulated-driving amplitude equation all predict essentially the same ODTL for thermal noise. These ODTL's are also very close to the one predicted by the generalized Lorenz model previously introduced by the authors [13]. The main feature that all these model equations share is that they are derived from the start for time-periodic driving, which leads in all cases to a nontrivial convection threshold. This feature clearly sets them apart from the usual SH or amplitude equations, in whose derivation the driving is assumed to be static, and its time dependence is introduced *a posteriori* [1]. Their convection onset is thus trivial, and all of them predict essentially the same thermal-noise ODTL that is shown in Fig. 2 for the SH equation. This suggests the likely hypothesis that any model equation correctly incorporating the driving time dependence will predict approximately the same ODTL as the ones discussed here. However, it must be emphasized that the ODTL predicted from Eq. (52) is probably not meaningful, since for a significant part of the parameter range it is used well beyond its validity range $\tilde{\Delta}^2 g^{(2)} \ll 1$ [11].

On the other hand, the mentioned model equations treat convective structure in very different ways: The model introduced here and its reduction to a Swift-Hohenberg-like equation fully respect the translational and rotational symmetry of the hydrodynamic equations, so any structure appearing above the convective threshold is spontaneously selected by the model dynamics. The Lorenz model and the amplitude equation instead select *a priori* some preferred convective structure, so they do not allow for *spontaneous* symmetry breaking. Thus, in spite of the numerical coincidence of the ODTL's predicted by all these models, we think that the one introduced here is conceptually more appealing.

These model equations also differ in their attention to the inertial effects embedded in the hydrodynamic equations. The periodic-driving amplitude equation of Ref. [11] assumes a common amplitude for both the temperature and vertical velocity fields, which leads to a *single* first-order differential equation for this amplitude. This is in the same standing as the hypothesis of a single order parameter used in the derivation of the SH equation [9]. For the periodic-driving amplitude equation this leads in particular to the temperature and vertical velocity fields having the same dependence on the horizontal coordinates. This is clearly not the case for the fields in Eqs. (26) (though it is true for the Lorenz model [13]), which even without noise have solutions in which the difference in horizontal coordinate dependence does not reduce to a mere global phase factor. The inclusion of noise further enhances this effect, in a way that is not simple to include in the scheme of amplitude or SH equations. It is interesting to note that for the parameter ranges of the experiment by Meyer, Ahlers, and Cannell [3]—which in particular has a moderate Prandtl number—the magnitude of the noise in $\tilde{u}_{z0}$ is much smaller than in $\tilde{\theta}_0$ in Eqs. (26). This makes Eqs. (26) very reminiscent of a (spatially extended) Kramers equation, which is well known to be reducible to a single Langevin equation only for large damping, corresponding in our case to large Prandtl numbers and a driving not too near the convective threshold.

Other aspect deserving consideration is that the periodic-driving amplitude equation (52) reduces for $\delta \to 0$ to the corresponding amplitude equation for static forcing [2], as is evident from its coefficients dependence with $\tilde{\Delta}$ in Eqs. (C15). In particular the value for the nonlinear coupling coefficient reduces to the same one in the SH equation [1]. However, this value for g is much smaller than the experimentally observed values [2], even accounting for the difference in Prandtl number and cell aspect ratio between the experiments of Refs. [2] and [3]. From the measurements by Ahlers *et al.* [2] of vertical heath flux versus driving in the static case around the convection threshold, it is clear that the value for g in the SH or the static amplitude equations is too small even in the static case. The same conclusion can be drawn from numerical simulations of the SH equation [25]. Thus a proper model of periodic-driving convection should *not* reduce in the static case to the static amplitude or SH equations with their static coefficients, but instead to similar equations with an appropriately larger nonlinear coupling. This is precisely the case of Eq. (50), which turns out to give a value for g very similar to the experimental ones.

As is seen in Figs. 1, 2, and 3, thermal noise is still insufficient for the predicted ODTL to match the experimental values of Ref. [3]. However, the predicted ODTL is still much nearer to the experimental values than that predicted from the MF approximation of the SH equation [19] (or from equivalent model equations) shown in Fig. 2. It can be shown that a noise intensity ~ 250 times the thermodynamic one needs to be used for the SH equation to predict an ODTL near the one predicted by the present model for thermal noise. Hence the consistent incorporation of the driving time-dependence reduces the misfit with the experimental values from a factor $\sim 5\times 10^4$ for the noise in the SH equation [19] to a much smaller factor ~ 200. This is a step forward, as it drastically reduces the requirements on any mechanism proposed to account for the remaining misfit.

It should be noted that even for the present model, fluctuations in the temperature of the Rayleigh-Bénard cell plates are very unlikely to provide the needed corrections. Recasting the results of Ref. [19] in terms of multiplicative noise in Eq. (50) shows that fluctuation intensities comparable to that allowed in experimental settings [2,3,5] leave the predicted ODTL unchanged, as is the case for the SH equation.

D. Concluding remarks

In this work we derived a set of evolution equations (26) for the velocity and temperature fields u_z and θ in a Rayleigh-Bénard cell with time-dependent forcing. The approach we implemented is fairly general, and can in principle be extended to a number of pattern-forming systems with spontaneous symmetry breaking. The derivation relied heavily on two simplificating assumptions: the mean field approximation and the truncated expansion in vertical eigenfunctions.

The MF approximation has been previously applied to the SH equation [19] and to the Lorenz model with noise [13]. In all cases in which comparison with Monte Carlo integration of the corresponding full stochastic equations was available, it has proved to be a very reliable method of computing self-correlations. In particular, ODTL's computed from the MF approximation to the Lorenz model with noise [13] differ from the Monte Carlo results by 2–3 %. The coincidence of the MF results for the SH equation with stochastic simulations, like those in Ref. [26], is also striking. The technical advantage of the MF approximation is that the ensemble averages of the fields are independent of the horizontal coordinates, enabling the use of linear analysis methods like Fourier transforms without the introduction of cumbersome convolution terms. In this aspect, Eqs. (26) are treated as *linear* equations for the fields. The introduction of the unknown field averages is not a complication, as long as all one is interested in are average quantities like the fields' self-correlations or structure factors: the effective linearization of Eqs. (26) allows these quantities to be obtained solving a closed, self-consistent system of equations like Eqs. (41) and (42).

The truncated expansion in vertical eigenfunctions is justified both by the large (infinite, in our case) aspect ratio of typical Rayleigh-Bénard cells, and by the smallness of the driving $R(t)/R_c-1$ in the situations considered here, which constrain the amplitudes of higher-order vertical modes to remain small at all times [1,10,11]. For a driving well above the convective threshold it is likely that more vertical modes will have to be retained. This would require a treatment of the vertical eigenfunctions more careful than the one given here, like, e.g., the one given by Cross [27]. It is worth noting that for the truncated expansion (23), the evolution equation for $\overline{u_{z0}}(\mathbf{x},t)$ would be linear in the fields even without assuming the MF approximation.

It must be emphasized that, in contrast with other approaches like the introduction of amplitude equations or the Lorenz model, our scheme preserves the full translational and rotational symmetry of the Oberbeck-Boussinesq equations. No symmetry-breaking pattern is introduced in the derivation, nor do asymmetric scaling properties need to be assumed for their spatial and temporal variations [12]. This is conceptually satisfying, since it is well known that symmetry breaking in these systems occurs spontaneously, rather than by external action. Though a rotationally covariant amplitude equation has been recently derived by Graham [12], even if the perturbative expansion developed by Schmitt and Lücke [11] could be extended in this way it will undoubtedly lead to a very involved calculation, and the necessity of using it for $\tilde{\Delta}g^{(2)}\sim 1$ casts doubt about its possible usefulness in analyzing the experiments of Ref. [3].

On the other hand, the approach presented here retains a full rotational (and translational) symmetry in the horizontal plane, even at times at which the system is well above the convective threshold. The mean square values of the fields at these times are (correctly) far from zero in the vicinity of $k=q_c$, but the structure factors present no trace of rolls, hexagons, or other symmetry-breaking structures. Part of these behavior is due to the presence of noise, in the same sense that the (asymptotic) probability distribution for a noisy system above a pitchfork bifurcation retains the symmetry of the potential, while the deterministic solutions spontaneously break it [28]. But in the present case the MF approximation strongly contributes to this effect: the assumption that the ensemble averages are spatially uniform is correct, but the macroscopic states experimentally observed do not correspond to these averages. The experimental observation time scale, while long compared with the time scale of the thermodynamic noise, is much shorter than the times needed for this noise to induce the system to switch between macroscopically distinguishable convective states, at least while well-developed convection persists. This can be seen, e.g., in the Fourier-transformed shadowgraphs obtained recently by Wu, Ahlers, and Cannell [5] for static forcing: below threshold the structure factor has full rotational invariance, showing an annular maximum at $k=q_c$, but above threshold it shows six very localized maxima with hexagonal symmetry (though still for $k=q_c$). Given the symmetry of this experimental setting, it is to be expected that shadowgraphs taken over a long enough time will show these peaks to drift under the influence of noise until they uniformly cover the cycle $k=q_c$, corresponding to the rotation of the convective pattern over all of its equivalent angular orientations; but this time scale is far longer than the experimental one.

This same translational and rotational symmetry precludes the inclusion of other disordering effects, such as the *structural* disorder introduced through defect nucleation (this is also true for any model assuming a given ordered pattern in the convective state, such as the Lorenz model [10] or the amplitude equation [11]). It is currently well known [1,30], that under suitable circumstances, the spatially inhomogeneous state spontaneously emerging above threshold does not show a perfect (periodic) array of rolls or cells, but a collection of ordered domains with no overall correlation. The underlying reason for this is that the homogeneous state bifurcates to the structured state *independently* at many locations, so even if the emerging state has the same structure everywhere (e.g., rolls), it is improbable for these structures to emerge with the same orientation or spatial phase at all locations. This introduces an additional source of ''randomness'' (besides thermal noise) in the bifurcation to a structured state: it appears much less probable for the very same

TABLE I. Coefficients for the vertical eigenfunctions.

n	R_n	α_1	Reα_2	Imα_2	c_{n1}, c'_{n1}	Rec_{n2}[a]	Imc_{n2}[a]	Rec'_{n2}[a]	Imc'_{n2}[a]
0	1707.76	3.973 70	2.125 87	5.194 39	1.475 27	8.907 25	0.098 06	−4.538 55	7.664 87
1	24 988.4	7.256 94	3.664 40	7.370 66	1.426 99	2.365 89	−2.369 26	0.868 90	3.233 55
2	171 763	10.4348	5.231 09	9.817 03	1.419 07	−0.002 43	−1.013 82	0.879 21	0.504 80
3	756 886	13.5913	6.802 15	12.3773	1.416 50	−0.202 07	−0.201 14	0.275 23	−0.074 43

[a]($\times 10^{-2}$)

pattern of domains to be reproduced from one cycle to the next, than to reproduce the same perfect pattern. Even for a static experiment there is no guarantee that the domains will eventually heal in a perfect pattern (some topological defects may survive indefinitely [1]), and in experiments like the one by Meyer, Ahlers, and Cannell [3] the control parameter is cycled again below threshold sooner than the pattern healing can proceed. Thus it could be expected that the inclusion of the effects of defect nucleation would lead to a predicted ODTL for thermal noise nearer to the experimental data than the ones presented here. Work along these lines is in progress.

ACKNOWLEDGMENTS

This work was supported in part by CONICOR Grant No. AIF-3854/95, SeCyT-UNC Grant No. 89/96, and CONICET Grant No. 653/1997.

APPENDIX A: VERTICAL EIGENFUNCTIONS

We perform a standard linear stability analysis, looking for the marginally stable solutions of the linearized, noiseless version of Eqs. (10) with *static* forcing; that is, we look for solutions of

$$0=\sigma\nabla^4 u_i+\sigma(\delta_{iz}\nabla^2-\partial_i\partial_z)\theta, \tag{A1a}$$

$$0=\nabla^2\theta+Ru_z. \tag{A1b}$$

Here we made use of the fact that the static conduction profile satisfies

$$0=\partial_z^2 T^c, \quad T^c(-\tfrac{1}{2})=T^l, \quad T^c(\tfrac{1}{2})=T^u, \tag{A2}$$

with solution

$$T^c(z)=(\tfrac{1}{2}-z)T^l+(\tfrac{1}{2}+z)T^u, \tag{A3}$$

and defined $R=T^l-T^u$. The pair of equations for u_z and θ in Eq. (A1) is closed. Fourier transforming from $\mathbf{x}=(x,y)$ to $\mathbf{q}=(q_x,q_y)$ gives

$$0=\sigma(\partial_z^2-q^2)^2\tilde{u}_z-\sigma q^2\tilde{\theta}, \tag{A4a}$$

$$0=(\partial_z^2-q^2)\tilde{\theta}+R\tilde{u}_z, \tag{A4b}$$

with BC's $\tilde{u}_z(\mathbf{q},z)=\partial_z\tilde{u}_z(\mathbf{q},z)=\tilde{\theta}(\mathbf{q},z)=0$ at $z=\pm\frac{1}{2}$ (the tilde denotes the transformed fields). This pair of ordinary differential equations can be cast as a single equation for either $\tilde{u}_z$ or $\tilde{\theta}$,

$$(\partial_z^2-q^2)^3\tilde{u}_z+q^2R\tilde{u}_z=0, \tag{A5a}$$

$$(\partial_z^2-q^2)^3\tilde{\theta}+q^2R\tilde{\theta}=0, \tag{A5b}$$

with BC's $\tilde{u}_z=\tilde{u}'_z=\tilde{u}^{iv}_z-2q^2\tilde{u}''_z=0$ and $\tilde{\theta}=\tilde{\theta}''=\tilde{\theta}''''-q^2\tilde{\theta}'=0$, respectively, at $z=\pm\frac{1}{2}$ (the primes denote differentiation with respect to z). We will assume $q^2>0$, $R>0$.

Now we must find the real eigenfunctions and the eigenvalues of Eq. (A5). It is straightforward to see that the differential operator in Eq. (A5a), with its boundary conditions, is not Hermitian. Neither is the operator in Eq. (A5b), with its boundary conditions. Hence the left and right eigenfunctions of Eq. (A5a) will not be the same, and neither will those of Eq. (A5b). However, it can be verified by partial integration that for any two functions $f(z)$ satisfying the BC's of Eq. (A5a), and $g(z)$ satisfying the BC's of Eq. (A5b),

$$\int_{-1/2}^{1/2} g(z)(\partial_z^2-q^2)^3 f(z)dz=\int_{-1/2}^{1/2} f(z)(\partial_z^2-q^2)^3 g(z)dz. \tag{A6}$$

So we see that the right eigenfunctions of Eq. (A5a) will be identical (apart of multiplicative constants) to the left eigenfunctions of Eq. (A5b), and vice versa. Hence it suffices to find the right eigenfunctions for both Eqs. (A5).

We look for solutions of the form $\tilde{\theta}=e^{i\alpha z}$, $\tilde{u}_z=e^{i\alpha z}$. Substituting in Eqs. (A5), a characteristic equation results in both cases,

$$(\alpha^2+q^2)^3=q^2R, \tag{A7}$$

which has six complex solutions $\pm\alpha_l$, $l=1$, 2, and 3, with

$$\alpha_1(q,R)=\sqrt{(q^2R)^{1/3}-q^2}, \tag{A8a}$$

$$\alpha_2(q,R)=\sqrt{\tfrac{1}{2}(-1+i\sqrt{3})(q^2R)^{1/3}-q^2}, \tag{A8b}$$

$$\alpha_3(q,R)=\sqrt{\tfrac{1}{2}(-1-i\sqrt{3})(q^2R)^{1/3}-q^2}. \tag{A8c}$$

Note that $\alpha_3=\alpha_2^*$ (the asterisk denotes complex conjugation). From the fact that both the differential equations (A5) and their boundary conditions are even in z, we see that the

eigenfunctions must have definite parity. Moreover, they will depend on the wave number **q** only through its modulus q, as expected from the rotational invariance of Eqs. (A1) in the (x,y) plane. The eigenfunctions will also depend on R, as a parameter.

The eigenfunctions can be cast in the forms

$$\tilde{u}_z(q,z;R)=c_1'\begin{Bmatrix}\cos\\ \sin\end{Bmatrix}[\alpha_1(q,R)z]+\left[c_2'\begin{Bmatrix}\cos\\ \sin\end{Bmatrix}[\alpha_2(q,R)z]+\text{c.c.}\right], \quad \text{(A9a)}$$

$$\tilde{\theta}(q,z;R)=c_1\begin{Bmatrix}\cos\\ \sin\end{Bmatrix}[\alpha_1(q,R)z]+\left[c_2\begin{Bmatrix}\cos\\ \sin\end{Bmatrix}[\alpha_2(q,R)z]+\text{c.c.}\right], \quad \text{(A9b)}$$

where the cosines and sines correspond respectively to even and odd eigenfunctions, and we assume that c_1 and c_1' are real. Substituting the even form of $\tilde{\theta}(q,z;R)$ in the BC's of (A5b) gives a homogeneous system of three linear equations for the coefficients c_1, c_2, and c_2^*, whose coefficient matrix is

$$\mathsf{M}_e(q,R)=\begin{pmatrix}\cos(\alpha_1/2) & \cos(\alpha_2/2) & \cos(\alpha_3/2)\\ -\alpha_1^2\cos(\alpha_1/2) & -\alpha_2^2\cos(\alpha_2/2) & -\alpha_3^2\cos(\alpha_3/2)\\ \alpha_1(\alpha_1^2+q^2)\sin(\alpha_1/2) & \alpha_2(\alpha_2^2+q^2)\sin(\alpha_2/2) & \alpha_3(\alpha_3^2+q^2)\sin(\alpha_3/2)\end{pmatrix}. \quad \text{(A10)}$$

Substituting the even form of $\tilde{u}_z(q,z;R)$ in the BC's of Eq. (A5a) gives a completely equivalent system, with a coefficient matrix

$$\mathsf{M}_e'(q,R)=\begin{pmatrix}\cos(\alpha_1/2) & \cos(\alpha_2/2) & \cos(\alpha_3/2)\\ -\alpha_1\sin(\alpha_1/2) & -\alpha_2\sin(\alpha_2/2) & -\alpha_3\sin(\alpha_3/2)\\ \alpha_1^2(\alpha_1^2+2q^2)\cos(\alpha_1/2) & \alpha_2^2(\alpha_2^2+2q^2)\cos(\alpha_2/2) & \alpha_3^2(\alpha_3^2+2q^2)\cos(\alpha_3/2)\end{pmatrix}. \quad \text{(A11)}$$

The corresponding coefficient matrices for the odd forms of $\tilde{\theta}(q,z;R)$ and $\tilde{u}_z(q,z;R)$ are

$$\mathsf{M}_o(q,R)=\begin{pmatrix}\sin(\alpha_1/2) & \sin(\alpha_2/2) & \sin(\alpha_3/2)\\ -\alpha_1^2\sin(\alpha_1/2) & -\alpha_2^2\sin(\alpha_2/2) & -\alpha_3^2\sin(\alpha_3/2)\\ -\alpha_1(\alpha_1^2+q^2)\cos(\alpha_1/2) & -\alpha_2(\alpha_2^2+q^2)\cos(\alpha_2/2) & -\alpha_3(\alpha_3^2+q^2)\cos(\alpha_3/2)\end{pmatrix} \quad \text{(A12)}$$

and

$$\mathsf{M}_o'(q,R)=\begin{pmatrix}\sin(\alpha_1/2) & \sin(\alpha_2/2) & \sin(\alpha_3/2)\\ \alpha_1\cos(\alpha_1/2) & \alpha_2\cos(\alpha_2/2) & \alpha_3\cos(\alpha_3/2)\\ \alpha_1^2(\alpha_1^2+2q^2)\sin(\alpha_1/2) & \alpha_2^2(\alpha_2^2+2q^2)\sin(\alpha_2/2) & \alpha_3^2(\alpha_3^2+2q^2)\sin(\alpha_3/2)\end{pmatrix}, \quad \text{(A13)}$$

respectively.

The solvability conditions $\det\mathsf{M}_e(q,R)=0$ and $\det\mathsf{M}_e'(q,R)=0$ both give the same equation relating q and R, which we will not write here for brevity. Numerical analysis of this equation finds a succession of curves on the q-R plane where $\det\mathsf{M}_e$ vanishes. The solvability conditions $\det\mathsf{M}_o(q,R)=0$ and $\det\mathsf{M}_o'(q,R)=0$ are equivalent too, and define another set of curves on the q-R plane, interspersed with the first ones. The first five of these curves are shown in Fig. 4. Considered as functions $R_i(q)$, $i=0,1,2,\ldots$ (the even and odd indexes correspond to even and odd eigenfunctions, respectively), each of these curves has a minimum for progressively increasing values $q_0<q_1<q_2<\cdots$ of q, from which it branches upwards in the q-R plane. The point $(q_0,R_0(q_0))$ corresponds to the well-known values of the critical wave number $q_0=q_c=3.11632$ and the critical Rayleigh number $R_0(q_0)=R_c=1707.76$, at which the first convective mode of the OB equations destabilizes. For $R<R_c$ all modes are stable, and the system is in a purely conductive state. For any given value of R, all values of q such that $R_i(q)<R$ correspond to linearly unstable modes of the OB equations with wavelength q.

To construct a complete, orthonormal set of vertical eigenfunctions, we must choose a fixed value for q. (Though it could seem conceptually more appealing, choosing for each eigenfunction the corresponding critical value q_i for q would not give mutually orthogonal left and right eigenfunctions, as they will belong in this case to different differential equations.) We select, as usual, $q=q_c$, and define $R_i=R_i(q_c)$. The first four values R_i are shown in Table I, as well as $\alpha_1(q_c,R_i)$ and $\alpha_2(q_c,R_i)$. Accordingly, we take as our velocity and temperature right eigenfunctions

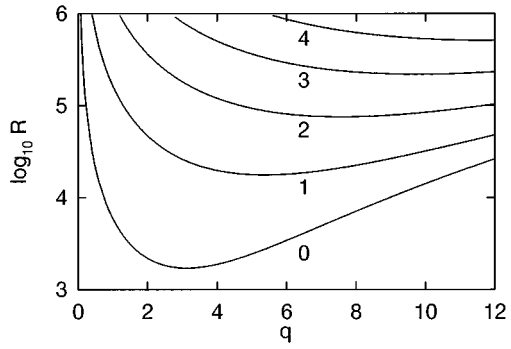

FIG. 4. Curves $R_i(q)$, $i=0,\ldots,4$. The minimum of $R_0(q)$ defines the point (q_c,R_c).

$$U_{zi}(z)=\tilde{u}_z(q_c,z;R_i)=c'_{i1}\begin{Bmatrix}\cos\\ \sin\end{Bmatrix}[\alpha_1(q_c,R_i)z] + \left[c'_{i2}\begin{Bmatrix}\cos\\ \sin\end{Bmatrix}[\alpha_2(q_c,R_i)z]+\text{c.c.}\right], \quad \text{(A14a)}$$

$$\Theta_i(z)=\tilde{\theta}(q_c,z;R_i)=c_{i1}\begin{Bmatrix}\cos\\ \sin\end{Bmatrix}[\alpha_1(q_c,R_i)z] + \left[c_{i2}\begin{Bmatrix}\cos\\ \sin\end{Bmatrix}[\alpha_2(q_c,R_i)z]+\text{c.c.}\right]. \quad \text{(A14b)}$$

The corresponding coefficients c_{ij} and c'_{ij} are the solutions of the equation systems

$$\mathsf{M}(q_c,R_i)\begin{pmatrix}c_{i1}\\ c_{i2}\\ c^*_{i2}\end{pmatrix}=0, \quad \mathsf{M}'(q_c,R_i)\begin{pmatrix}c'_{i1}\\ c'_{i2}\\ c'^*_{i2}\end{pmatrix}=0\,, \quad \text{(A15)}$$

respectively, where M stands for either M_e or M_o according to the parity of i, and similarly for M'. The coefficients c_{ij} and c'_{ij} can be selected to give mutually normalized eigenfunctions. Their values for $i=0$, 1, 2, and 3 are shown in Table I. With no generality loss we have furthermore set $c'_{1j}=c_{1j}$.

The first four normalized eigenfunctions $U_{zi}(z)$ and $\Theta_i(z)$ are plotted in Fig. 5. They can be shown to form a mutually orthonormal set, that is

$$\int_{-1/2}^{1/2} U_{zi}(z)\Theta_j(z)dz=\delta_{ij}\,. \quad \text{(A16)}$$

Note that $U_{zi}(z)$ and $\Theta_i(z)$ have the parity of their index, and show i nodes between $z=-\frac{1}{2}$ and $\frac{1}{2}$, as expected.

APPENDIX B: EXPANSIONS IN VERTICAL EIGENFUNCTIONS

In this appendix we derive the projections over the relevant vertical eigenfunctions of the instantaneous conductive profile and of the noise amplitudes.

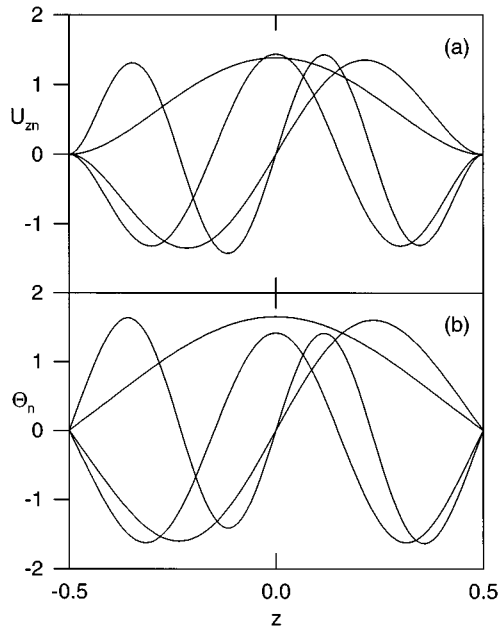

FIG. 5. Vertical eigenfunctions $U_{zn}(z)$ (a) and $\Theta_n(z)$ (b), $n=0,\ldots,3$. The nth eigenfunction has n nodes in $-\frac{1}{2}\leqslant z\leqslant\frac{1}{2}$.

1. Conductive profile

The instantaneous conductive profile is the solution of the heat conduction equation (6) with the instantaneous, inhomogeneous BC's (7). It is convenient to separate it as a linear profile plus a deviation from linearity $S(z,t)$, i.e.,

$$T^c(z,t)=T_u+(1/2-z)R(t)+S(z,t), \quad \text{(B1)}$$

where $R(t)$ is the instantaneous Rayleigh number (8). The equation for S is then

$$\partial_t S=\partial_z^2 S-(1/2-z)\partial_t R(t), \quad \text{(B2)}$$

with homogeneous BC's at $z=\pm\frac{1}{2}$. Substituting the truncated expansion

$$S(z,t)=\Theta_0(z)S_0(t)+\Theta_1(z)S_1(t), \quad \text{(B3)}$$

multiplying by $U_{z1}(z)$, and integrating over z, we obtain

$$\dot{S}_1(t)=-\{U'_{z1}\Theta'_1\}S_1(t)-\{U_{z1}(1/2-z)\}\Delta\omega\,\sin(\omega t), \quad \text{(B4)}$$

where we used the orthonormality relation $\{U_{zi}\Theta_j\}=\delta_{ij}$. We also set $\{U_{z1}\Theta''_0\}=0$ because of the eigenfunction's parity, and $\{U_{z1}\Theta''_1\}=-\{U'_{z1}\Theta'_1\}$ by partial integration. The positivity of $\{U'_{z1}\Theta'_1\}$ ensures the existence of a periodic long-time asymptotic solution, which is

$$S_1(t)=\Delta\omega\{zU_{z1}\}\frac{\{U'_{z1}\Theta'_1\}\sin(\omega t)-\omega\,\cos(\omega t)}{\{U'_{z1}\Theta'_1\}^2+\omega^2}. \quad \text{(B5)}$$

Here we used the parity of U_{z1} to set $\{U_{z1}\}=0$. The numerical values of $\{zU_{z1}\}$ and $\{U'_{z1}\Theta'_1\}$ are given in Table II. An expression for $S_0(t)$ can be found in the same way, but we do not show it here since S_0 does not enter Eqs. (26).

TABLE II. Inner products of the vertical eigenfunctions.

$\{U_{z0}U_{z0}\}$	0.781 901	$\{U'_{z0}U'_{z0}\}$	9.340 89
$\{\Theta_0\Theta_0\}$	1.297 86	$\{\Theta'_0\Theta'_0\}$	12.8977
$\{\Theta''_0\Theta''_0\}$	135.587	$\{U'_{z0}\Theta'_0\}$	10.2284
$\{U^{iv}_{z0}\Theta_0\}$	551.073	$\{U'_{z1}\Theta'_1\}$	40.8770
$\{U_{z0}U_{z0}\Theta'_1\}$	4.966 78	$\{U_{z0}\Theta_0U'_{z1}\}$	4.803 06
$\{zU_{z1}\}$	0.173 930		

2. Noise terms

The noise term in Eq. (19b) is

$$\mathcal{Q}(\mathbf{r},t)=-\frac{\partial}{\partial r_i}q_i(\mathbf{r},t), \tag{B6}$$

where $q_i(\mathbf{r},t)$ are zero-mean Gaussian white noise fields with self-correlations given by Eq. (2b), and r_i stands for the ith component of $\mathbf{r}$. Then

$$\langle \mathcal{Q}(\mathbf{r},t)\mathcal{Q}(\mathbf{r}',t')\rangle = c_q\delta(t-t')\frac{\partial}{\partial r_i}\frac{\partial}{\partial r'_i}\delta(\mathbf{r}-\mathbf{r}'). \tag{B7}$$

For any set of test functions in $-\infty\leqslant x,y\leqslant\infty$, $-\frac{1}{2}\leqslant z\leqslant\frac{1}{2}$ satisfying the temperature vertical BC's (11), we have $\partial_{x'}\delta(x-x')=-\partial_x\delta(x-x')$, so we immediately obtain

$$\langle \mathcal{Q}(\mathbf{r},t)\mathcal{Q}(\mathbf{r}',t')\rangle = -c_q\delta(t-t')\nabla^2\delta(\mathbf{r}-\mathbf{r}') \tag{B8}$$

for any set of test functions in $-\infty\leqslant x,y\leqslant\infty$, $-\frac{1}{2}\leqslant z\leqslant\frac{1}{2}$ satisfying the velocity vertical BC's (11). Fourier transforming from **x** to **k** gives

$$\langle \widetilde{\mathcal{Q}}^*(\mathbf{k},z,t)\widetilde{\mathcal{Q}}(\mathbf{k}',z',t')\rangle = (2\pi)^2c_q\delta(\mathbf{k}-\mathbf{k}')\delta(t-t')\times(k^2-\partial_z^2)\delta(z-z'). \tag{B9}$$

The noise term in Eq. (19a) is

$$\mathcal{S}_z(\mathbf{r},t)=\left(\delta_{zj}\frac{\partial}{\partial r_i}\frac{\partial}{\partial r_i}-\frac{\partial}{\partial r_z}\frac{\partial}{\partial r_j}\right)\frac{\partial}{\partial r_k}s_{jk}(\mathbf{r},t), \tag{B10}$$

where $s_{ij}(\mathbf{r},t)$ are zero-mean Gaussian white noise fields with self-correlations given by Eq. (2a). A thoroughly similar procedure leads to

$$\langle \mathcal{S}_z(\mathbf{r},t)\mathcal{S}_z(\mathbf{r}',t')\rangle = -c_s\delta(t-t')\nabla^4(\nabla^2-\partial_z^2)\delta(\mathbf{r}-\mathbf{r}). \tag{B11}$$

Fourier transforming from **x** to **k** gives

$$\langle \widetilde{\mathcal{S}}^*_z(\mathbf{k},z,t)\widetilde{\mathcal{S}}_z(\mathbf{k}',z',t')\rangle = (2\pi)^2c_s\delta(\mathbf{k}-\mathbf{k}')\delta(t-t')k^2\times(k^2-\partial_z^2)^2\delta(z-z'). \tag{B12}$$

The noise term in Eq. (26b) is defined as

$$\sqrt{D_\theta(k)}\,\widetilde{\xi}_\theta(\mathbf{k},t)=\widetilde{\mathcal{Q}}_0(\mathbf{k},t)=\int_{-1/2}^{1/2}U_{z0}(z)\widetilde{\mathcal{Q}}(\mathbf{k},z,t)dz, \tag{B13}$$

which shows that it too is a zero-mean Gaussian white noise field. Its self-correlation is then

$$\begin{aligned}\langle \widetilde{\mathcal{Q}}^*_0(\mathbf{k},t)\widetilde{\mathcal{Q}}_0(\mathbf{k}',t')\rangle &= (2\pi)^2c_q\delta(\mathbf{k}-\mathbf{k}')\delta(t-t')\\ &\times\int_{-1/2}^{1/2}dz\,U_{z0}(z)\int_{-1/2}^{1/2}dz'\,U_{z0}(z')\\ &\times(k^2-\partial_z^2)\delta(z-z')\\ &=(2\pi)^2c_q\delta(\mathbf{k}-\mathbf{k}')\delta(t-t')\\ &\times[\{U_{z0}U_{z0}\}k^2-\{U_{z0}U''_{z0}\}].\end{aligned} \tag{B14}$$

Integrating by parts the term $\{U_{z0}U''_{z0}\}$ to symmetrize the inner product, we obtain the result in Eqs. (27)–(28b).

The noise term in Eq. (26a) is defined as

$$\sqrt{D_u(k)}\,\widetilde{\xi}_u(\mathbf{k},t)=\widetilde{\mathcal{S}}_{z0}(\mathbf{k},t)=\frac{1}{k^2+\{U'_{z0}\Theta'_0\}}\times\int_{-1/2}^{1/2}\Theta_0(z)\widetilde{\mathcal{S}}_z(\mathbf{k},z,t)dz, \tag{B15}$$

then

$$\langle \widetilde{\mathcal{S}}^*_{z0}(\mathbf{k},t)\widetilde{\mathcal{S}}_{z0}(\mathbf{k}',t')\rangle = (2\pi)^2c_s\delta(\mathbf{k}-\mathbf{k}')\delta(t-t')\frac{k^2}{[k^2+\{U'_{z0}\Theta'_0\}]^2}\int_{-1/2}^{1/2}dz\;\Theta_0(z)\int_{-1/2}^{1/2}dz'\,\Theta_0(z')(k^2-\partial_z^2)^2\delta(z-z')$$

$$=(2\pi)^2c_s\delta(\mathbf{k}-\mathbf{k}')\delta(t-t')k^2\frac{\{\Theta_0\Theta_0\}k^4-2\{\Theta_0\Theta''_0\}k^2+\{\Theta_0\Theta^{iv}_0\}}{[k^2+\{U'_{z0}\Theta'_0\}]^2}. \tag{B16}$$

Integrating by parts to symmetrize the inner products, we obtain the result in Eqs. (27)–(28a).

APPENDIX C: ALTERNATIVE MODELS

1. Reduction to a Swift-Hohenberg-like equation

It is well known that for a large σ and the small amplitude δ of the forcing, the Lorenz model of Refs. [10,13] reduces to a first-order amplitude equation [29]. Thus it is of interest to study the same limit for Eqs. (26).

Closely following the procedure for the Lorenz model, we first set

$$\widetilde{\theta}_0(\mathbf{k},t)=\frac{1}{\gamma_{u\theta}(k)}[-\partial_t\widetilde{u}_{z0}(\mathbf{k},t)-\gamma_{uu}(k)\widetilde{u}_{z0}(\mathbf{k},t)+\sqrt{D_u(k)}\,\widetilde{\xi}_u(\mathbf{k},t)], \tag{C1}$$

which follows from Eq. (26b). Using this and Eq. (37), we can integrate out $\langle \overline{\theta_1} \rangle$ in Eqs. (26) to obtain

$$\langle \overline{\theta_1} \rangle = \langle \overline{u_{z0}^2} \rangle + \langle M[\widetilde{u}_{z0}] \rangle, \tag{C2}$$

where M is a memory term exactly like the one in Ref. [10], which is negligible for small modulation and near the (static) convective threshold (i.e., for $\epsilon_0 \ll 1$). Substituting in Eq. (26a) and taking $\sigma \gg 1$, we obtain

$$\begin{aligned} &- \frac{\gamma_{uu}(k)+\gamma_{\theta\theta}(k)}{\gamma_{u\theta}(k)} \partial_t \widetilde{u}_{z0}(\mathbf{k},t) \\ &= -\Bigg[- \frac{\gamma_{uu}(k)\gamma_{\theta\theta}(k)}{\gamma_{u\theta}(k)} - \{U_{z0}U_{z0}\}R(t) + \{U_{z0}U_{z0}\Theta_1'\} \\ &\quad \times [S_1(t) + \langle \overline{u_{z0}^2} \rangle] \Bigg] \widetilde{u}_{z0}(\mathbf{k},t) + \sqrt{D_\theta(k)}\, \widetilde{\xi}_\theta(\mathbf{k},t) \\ &\quad - \frac{\gamma_{\theta\theta}(k)}{\gamma_{u\theta}(k)} \sqrt{D_u(k)}\, \widetilde{\xi}_u(\mathbf{k},t). \end{aligned} \tag{C3}$$

In writing this equation, we neglected terms which become small for $\sigma \gg 1$, in particular a second-order time derivative of $\widetilde{u}_{z0}$ on the left hand side, and the memory term $\langle M \rangle$. Defining

$$\tau_0 = - \frac{\gamma_{uu}(q_c)+\gamma_{\theta\theta}(q_c)}{\gamma_{u\theta}(q_c)\{U_{z0}U_{z0}\}R_c}, \tag{C4}$$

we rewrite Eq. (C3) as

$$\begin{aligned} &\tau_0 \partial_t \widetilde{u}_{z0}(\mathbf{k},t) \\ &= \Bigg[- \tau_0 \frac{\gamma_{uu}(k)\gamma_{\theta\theta}(k) + \gamma_{u\theta}(k)\{U_{z0}U_{z0}\}R_c}{\gamma_{uu}(k)+\gamma_{\theta\theta}(k)} \\ &\quad - \tau_0 \frac{\gamma_{u\theta}(k)\{U_{z0}U_{z0}\}R_c}{\gamma_{uu}(k)+\gamma_{\theta\theta}(k)} \Bigg(\epsilon_0 + \delta \cos(\omega t) \\ &\quad - \frac{\{U_{z0}U_{z0}\Theta_1'\}}{\{U_{z0}U_{z0}\}R_c} [S_1(t) + \langle \overline{u_{z0}^2} \rangle] \Bigg) \Bigg] \widetilde{u}_{z0}(\mathbf{k},t) \\ &\quad + \tau_0 \frac{\gamma_{\theta\theta}(k)\sqrt{D_u(k)}\, \widetilde{\xi}_u(\mathbf{k},t) - \gamma_{u\theta}(k)\sqrt{D_\theta(k)}\, \widetilde{\xi}_\theta(\mathbf{k},t)}{\gamma_{uu}(k)+\gamma_{\theta\theta}(k)}. \end{aligned} \tag{C5}$$

Now we expand the k-dependent coefficients of Eq.(C5) in powers of $k^2 - q_c^2$, in the same way as is done in the derivation of the SH equation in Ref. [9(a)]. In particular, we can see that

$$\begin{aligned} &- \tau_0 \frac{\gamma_{uu}(k)\gamma_{\theta\theta}(k) + \gamma_{u\theta}(k)\{U_{z0}U_{z0}\}R_c}{\gamma_{uu}(k)+\gamma_{\theta\theta}(k)} \\ &\simeq a(k^2-q_c^2) + b(k^2-q_c^2)^2 = \epsilon_1 - \chi^4 (k^2 - q_*^2)^2, \end{aligned} \tag{C6}$$

where we defined $\epsilon_1 = -a^2/(4b)$, $\chi^4 = -b$, and $q_*^2 = q_c^2 - a/(2b)$. The remaining coefficients are evaluated at $k = q_c$. Introducing $\widetilde{\psi}(\mathbf{k},t) = \tau_0 \widetilde{u}_{z0}(\mathbf{k},t)$, we obtain

$$\begin{aligned} \tau_0 \partial_t \widetilde{\psi}(\mathbf{k},t) &= [(\epsilon_0 + \epsilon_1) + \delta \cos(\omega t) + \epsilon_2 S_1(t) \\ &\quad - \chi^4 (k^2 - q_*^2)^2 - g \langle \overline{\psi^2} \rangle] \widetilde{\psi}(\mathbf{k},t) \\ &\quad + \sqrt{D}\, \widetilde{\xi}(x\mathbf{k},t), \end{aligned} \tag{C7}$$

where $\overline{\psi}$ is the Fourier antitransform of $\widetilde{\psi}$, and we defined

$$D = \tau_0^4 \frac{\gamma_{\theta\theta}^2(q_c) D_u(q_c) + \gamma_{u\theta}^2(q_c) D_\theta(q_c)}{[\gamma_{uu}(q_c) + \gamma_{\theta\theta}(q_c)]^2}. \tag{C8}$$

Here $\widetilde{\xi}(\mathbf{k},t)$ is a zero mean Gaussian white noise field with $\langle \widetilde{\xi}(\mathbf{k},t)\widetilde{\xi}(\mathbf{k}',t') \rangle = \delta(\mathbf{k}-\mathbf{k}')\delta(t-t')$. Fourier antitransforming leads to Eq. (50) of the main text.

For $\sigma = 6$, the numerical values of the coefficients are

$$\tau_0 = 5.409 \times 10^{-2},$$

$$\epsilon_1 = 2.022 \times 10^{-3},$$

$$\chi^4 = 3.839 \times 10^{-3},$$

$$q_*^2 = 10.44,$$

$$\epsilon_2 = -3.720 \times 10^{-3},$$

$$g = 1.271,$$

$$\sqrt{D} = 1.938 \times 10^{-5}.$$

The corresponding values for the SH equation are [19]

$$\tau_0 = 5.523 \times 10^{-2},$$

$$\epsilon_1 = 0,$$

$$\chi^4 = 3.810 \times 10^{-3},$$

$$q_*^2 = q_c^2,$$

$$\epsilon_2 = 0,$$

$$g = 0.2330,$$

$$\sqrt{D} = 0.3423 \times 10^{-5}.$$

2. Amplitude equation for time-periodic driving

For modulated Rayleigh-Bénard convection without noise a modified amplitude equation was derived by Schmitt and

Lücke [11]. They performed a systematic nonlinear perturbation of the hydrodynamic field equations using a Poincare-Lindstedt technique combined with a multiple-scale analysis, amounting to an expansion in powers of $(\epsilon-\epsilon_c)^{1/2}$, where ϵ_c is the reduced critical Rayleigh number for the convection onset in the presence of modulation. The expansion is introduced by assuming a parallel roll convective structure, defining the slow length and time scales $X_n=\eta^n x$ and $T_n=\eta^n t$ in addition to the fast variations in x and t, and setting

$$\epsilon-\epsilon_c=\eta\epsilon_1+\eta^2\epsilon_2+\cdots, \tag{C9a}$$

$$\mathbf{u}(\mathbf{r},t)=\eta\mathbf{u}_0(\mathbf{r},X,t,T)+\eta^2\mathbf{u}_1(\mathbf{r},X,t,T)+\cdots, \tag{C9b}$$

$$\theta(\mathbf{r},t)=\eta\theta_0(\mathbf{r},X,t,T)+\eta^2\theta_1(\mathbf{r},X,t,T)+\cdots, \tag{C9c}$$

where $X=\{X_1,X_2,\ldots\}$ and $T=\{T_1,T_2,\ldots\}$ denote all the slow length and time scales. The hydrodynamic fields are assumed to have the form

$$v(\mathbf{r},X,t,T)=A(X,T)f(\mathbf{r},t), \tag{C10}$$

where v stands for any of the fields u_i or θ, $f(\mathbf{r},t)$ is an eigenfunction taking into account the vertical BC's (including the time-periodic modulation) and the assumed convective structure, and

$$A(x,t)=\eta A_0(X,T)+\eta^2 A_1(X,T)+\cdots. \tag{C11}$$

Inserting these expansions into the Oberbeck-Boussinesq equations, the nonlinear problem is decomposed in a sequence of linear equations, each with inhomogeneities depending in general nonlinearly on previous ''coefficients'' (for details, see Ref. [11]).

Noise can be included in the above scheme by closely following the same steps as for the static-forcing amplitude equations, i.e., one must assume the appropriate scaling relationships for the noise correlations [8]. This leads to the noise being included in the solvability condition of the perturbative expansion at order η^3, which gives the first nonlinear amplitude combination in the form

$$\tau\partial_{T_2}A_0=[\xi^2\nabla_{X_1}^2+\epsilon_2-g|A_0|^2]A_0+\xi_{A_0}(X_1,T_2). \tag{C12}$$

Here $\xi_{A_0}(X_1,T_2)$ is a zero-mean Gaussian white noise field with self-correlation

$$\langle\xi_{A_0}^*(X_1,T_2)\xi_{A_0}(X_1',T_2')\rangle=D_{A_0}\delta(X_1-X_1')\delta(T_2-T_2'). \tag{C13}$$

Eliminating the slow auxiliary variables in favor of the original ones gives, for $A(x,t)$, the amplitude equation

$$\tau\partial_t A=[\xi^2\partial_x^2+\epsilon-\epsilon_c-g|A|^2]A+\xi_A(x,t), \tag{C14}$$

where the Gaussian white noise field $\xi_A(x,t)$ has intensity $D_A=D_{A_0}$,

$$\tau(\tilde{\Delta},\omega)=\tau^{(0)}[1+\tilde{\Delta}^2\tau^{(2)}(\omega)+O(\tilde{\Delta}^4)], \tag{C15a}$$

$$\xi^2(\tilde{\Delta},\omega)=\xi^{2(0)}[1+\tilde{\Delta}^2\xi^{2(2)}(\omega)+O(\tilde{\Delta}^4)], \tag{C15b}$$

$$g(\tilde{\Delta},\omega)=g^{(0)}[1+\tilde{\Delta}^2 g^{(2)}(\omega)+O(\tilde{\Delta}^4)], \tag{C15c}$$

$$\epsilon_c(\tilde{\Delta},\omega)=\tilde{\Delta}^2\epsilon_c^{(2)}(\omega)+O(\tilde{\Delta}^4), \tag{C15d}$$

$$k_c(\tilde{\Delta},\omega)=k_c^{(0)}[1+\tilde{\Delta}^2 k_c^{(2)}(\omega)+O(\tilde{\Delta}^4)], \tag{C15e}$$

and $\tilde{\Delta}=\Delta/(1+\epsilon_0)$ in terms of the main text parameters.

For free-slip BC's, the zero modulation amplitude parameters are

$$\tau^{(0)}=\frac{2}{3\pi^2}\frac{\sigma+1}{\sigma},\quad \xi^{2(0)}=\frac{8}{3\pi^2},$$
$$g^{(0)}=\frac{2}{3\pi^2},\quad k_c^{(0)}=\pi/\sqrt{2}, \tag{C16}$$

and the leading-order corrections are

$$\tau^{(2)}=\frac{\sigma^3}{(\sigma+1)^4}\mathcal{G}\left[1+\frac{1}{\sigma^2}\left(1+\frac{7}{6}\frac{\omega^2}{q_c^{(0)4}}\right)\right], \tag{C17a}$$

$$\xi^{2(2)}=\frac{1}{2}\frac{\sigma}{(\sigma+1)^2}\mathcal{G}\left(1+\frac{8\omega^2}{3(\sigma+1)^2q_c^{(0)4}}+\frac{3\omega^4}{(\sigma+1)^4q_c^{(0)8}}\right), \tag{C17b}$$

$$\epsilon_c^{(2)}=\frac{1}{2}\frac{\sigma}{(\sigma+1)^2}\mathcal{G}, \tag{C17c}$$

$$g^{(2)}\simeq\frac{1}{2}\frac{1}{(\omega\tau^{(0)})^2}, \tag{C17d}$$

$$k_c^{(2)}=-\frac{1}{4}\frac{\omega^2}{q_c^{(0)4}}\frac{\sigma}{(\sigma+1)^2}\mathcal{G}, \tag{C17e}$$

where $\mathcal{G}$ is given by

$$\mathcal{G}=\left[\left(1+\frac{\omega^2}{(\sigma+1)^2q_c^{(0)4}}\right)\left(1+\frac{\omega^2}{(2\pi)^4}\right)\right]^{-1}, \tag{C18}$$

and $q_c^{(0)2}=k_c^{(0)2}+\pi^2$. The noise intensity is

$$D_A=\frac{c_s k_c^2(k_c^2+\pi^2)^2}{(q_c^{(0)6}E)^2}. \tag{C19}$$

The coefficient E can be taken to be unity in all cases [11], since its correction to order $\tilde{\Delta}^2$ is very small. The coefficient c_s is the same as introduced in Eq. (2a).

Since the derivation of Schmitt and Lücke [11] relied on an expansion in vertical modes similar to the one used in the generalized Lorenz model of Ref. [10], the conversion to rigid boundary conditions may be performed in the same way as for this model. So the rigid BC coefficients are obtained by setting

$$\tau^{(0)}=\frac{\sigma+0.5117}{19.65\sigma}, \tag{C20a}$$

$$\xi^{2(0)}=0.148, \tag{C20b}$$

$$g^{(0)}=0.6995-0.0047\sigma^{-1}+0.0083\sigma^{-2}, \tag{C20c}$$

$$k_c^{(0)}=q_c=3.1163, \tag{C20d}$$

and replacing

$$q_c^{(0)4}\rightarrow q_c^4+\{U_{z0}'\Theta_0'\}q_c^2+\{\Theta_0 U_{z0}^{iv}\} \tag{C21}$$

in Eqs. (C17) and (C18). The noise intensity D_A becomes

$$D_A=\frac{c_s k_c^2(\{\Theta_0\Theta_0\}k_c^4+\{\Theta_0'\Theta_0'\}k_c^2+\{\Theta_0''\Theta_0''\})}{[(q_c^2+\{U_{z0}'\Theta_0'\})(q_c^4+\{U_{z0}'\Theta_0'\}q_c^2+\{\Theta_0 U_{z0}^{iv}\})]^2}. \tag{C22}$$

[1] M. C. Cross and P. C. Hohenberg, Rev. Mod. Phys. **65**, 851 (1993).
[2] G. Ahlers, M. C. Cross, P. C. Hohenberg, and S. Safran, J. Fluid Mech. **110**, 297 (1981).
[3] C. W. Meyer, G. Ahlers, and D. S. Cannell, Phys. Rev. Lett. **59**, 1577 (1987).
[4] C. W. Meyer, D. S. Cannell, and G. Ahlers, Phys. Rev. A **45**, 8583 (1992).
[5] M. Wu, G. Ahlers, and D. S. Cannell, Phys. Rev. Lett. **75**, 1743 (1995).
[6] J. Liu and G. Ahlers, Phys. Rev. Lett. **77**, 3126 (1996).
[7] K. M. Zaitsev and M. I. Shliomis, Zh. Éksp. Teor. Fiz. **59**, 1583 (1970) [Sov. Phys. JETP **32**, 866 (1971)].
[8] R. Graham, Phys. Rev. A **10**, 1762 (1974).
[9] (a) J. B. Swift and P. C. Hohenberg, Phys. Rev. A **15**, 319 (1977); (b) P. C. Hohenberg and J. B. Swift, *ibid.* **46**, 4773 (1992).
[10] G. Ahlers, P. C. Hohenberg, and M. Lücke, Phys. Rev. A **32**, 3493 (1985).
[11] S. Schmitt and M. Lücke, Phys. Rev. A **44**, 4986 (1991).
[12] R. Graham, Phys. Rev. Lett. **76**, 2185 (1996).
[13] O. Osenda, C. B. Briozzo, and M. O. Cáceres, Phys. Rev. E **55**, R3824 (1997).
[14] J. Kiezer, Phys. Fluids **21**, 198 (1978).
[15] H. van Beijeren and E. G. D. Cohen, J. Stat. Phys. **53**, 77 (1988).
[16] J. B. Swift and P. C. Hohenberg, Phys. Rev. Lett. **60**, 75 (1988).
[17] C. W. Meyer, G. Ahlers, and D. S. Cannell, Phys. Rev. A **44**, 2514 (1991).
[18] A. Becker, M. O. Cáceres, and L. Kramer, Phys. Rev. A **46**, R4463 (1992).
[19] O. Osenda, C. B. Briozzo, and M. O. Cáceres, Phys. Rev. E **54**, 6944 (1996).
[20] L. D. Landau and E. M. Lifshitz, *Statistical Physics* (Addison-Wesley, Reading, MA, 1969).
[21] K. Huang, *Statistical Mechanics*, 2nd ed. (Wiley, New York, 1987).
[22] H. Risken, *The Fokker-Planck Equation* (Springer-Verlag, Berlin, 1984).
[23] C. W. Gardiner, *Handbook of Stochastic Methods*, 2nd ed. (Springer-Verlag, Berlin, 1994).
[24] W. H. Press, S. A. Teukolsky, W. T. Vetterling, and B. P. Flannery, *Numerical Recipes*, 2nd ed. (Cambridge University Press, 1992).
[25] J. Viñals, H.-W. Xi, and J. D. Gunton, Phys. Rev. A **46**, 918 (1992).
[26] J. García-Ojalvo, A. Hernández-Machado, and J. M. Sancho, Phys. Rev. Lett. **71**, 1542 (1993).
[27] M. C. Cross, Phys. Fluids **23**, 1727 (1980).
[28] M. O. Cáceres, A. Becker, and L. Kramer, Phys. Rev. A **43**, 6581 (1991).
[29] M. C. Cross, Phys. Rev. A **25**, 1065 (1982); Y. Pomeau, S. Zalesky, and P. Manneville, *ibid.* **27**, 2710 (1983); M. C. Cross and A. C. Newell, Physica D **10**, 299 (1984).
[30] K. Takeyama, Prog. Theor. Phys. **63**, 91 (1980).